



UNIVERSIDADE ESTADUAL DE CAMPINAS  
SISTEMA DE BIBLIOTECAS DA UNICAMP  
REPOSITÓRIO DA PRODUÇÃO CIENTÍFICA E INTELLECTUAL DA UNICAMP

**Versão do arquivo anexado / Version of attached file:**

Versão do Editor / Published Version

**Mais informações no site da editora / Further information on publisher's website:**

<https://www.scielo.br/scielo.php?pid=S0103-64402019000500453>

**DOI: 10.1590/0103-6440201902463**

**Direitos autorais / Publisher's copyright statement:**

©2019 by USP/Fundação Odontológica de Ribeirão Preto. All rights reserved.

DIRETORIA DE TRATAMENTO DA INFORMAÇÃO

Cidade Universitária Zeferino Vaz Barão Geraldo

CEP 13083-970 – Campinas SP

Fone: (19) 3521-6493

<http://www.repositorio.unicamp.br>



# Analysis of Molecular Changes Induced By Mineral Trioxide Aggregate On sPLA2

Murilo B. Lopes<sup>1</sup>, Veronica C.G. Soares<sup>2</sup>, Fabio H.R. Fagundes<sup>3</sup>, Alcides Gonini-Junior<sup>1</sup>, Renan H. Kaneshima<sup>1</sup>, Ricardo D. Guiraldo<sup>1</sup>, Eduardo B.S. Diz-Filho<sup>4</sup>, Sandrine B. Berger<sup>1</sup>, Klissia R. Felizardo<sup>5</sup>, Marcelo L. dos Santos<sup>6</sup>

<sup>1</sup>Department of Restorative Dentistry, UNOPAR - Universidade Norte do Paraná, Londrina, PR, Brazil  
<sup>2</sup>Department of Pharmacy, UNIP - Universidade Paulista, Jundiaí, SP, Brazil  
<sup>3</sup>Health Sciences, UniAnchieta, Universidade Padre Anchieta, Jundiaí, SP, Brazil  
<sup>4</sup>Department of Biochemistry, UNICAMP - Universidade Estadual de Campinas, Campinas, SP, Brazil  
<sup>5</sup>Department of Dentistry, UNIPAR - Universidade Paranaense, Umuarama, PR, Brazil  
<sup>6</sup>Department of Chemistry, UFS - Universidade Federal de Sergipe, Aracaju, SE, Brazil

Correspondence: Dr. Murilo Baena Lopes, Rua Marselha, 183, 86041-140 Londrina, PR, Brasil. Tel: +55- 43-3371-7820. e-mail: baenalopes@gmail.com

The aim of this study was to analyze the effects of MTA on the structure and enzymatic activity of sPLA2 in order to provide subsidies for improvement in the formulation of the product. MTA powder was incubated for 60 min in the presence of sPLA2 and was analyzed by chromatography, electrospray mass (ESI-MS) and small-angle X-ray scattering (SAXS). It was found that the elution profile, retention time, and fragmentation of sPLA2 were altered after treatment with MTA. Calcium was the MTA component that most amplified the inflammatory signal. Significant interactions were found between MTA and sPLA2, which could aid in our understanding of the mechanisms of action of MTA during the inflammatory process and it may facilitate the structural modification of MTA, thereby improving its biological safety and consequently the rate of the treatment success.

Key Words: Inflammation, MTA, Calcium hydroxide, SAXS, Mass spectroscopy

## Introduction

Injuries to dentin may lead to an inflammatory reaction of the pulp. However, if left untreated, deeper cavity lesions may lead to pulp necrosis. In some cases, root perforations can result from resorptions and carious lesions. It should be repaired as quickly as possible with a biocompatible material able to seal the cavity, prevent bacterial invasion and inflammation development (1). Lesions of dental pulp show increased secretory phospholipase A2 (sPLA2) expression, indicating that inflammatory mediators are involved in disease progression (2). sPLA2 regulates the release of arachidonic acid from cellular phospholipids, resulting in the biosynthesis of eicosanoids during the inflammatory process so that these are not contained. Eicosanoids lead to necrosis of the pulp (3). The interaction between proteins and various types of macromolecules as a matter of considerable technological interest was already described (4).

Bioactivity is one of the most coveted properties of tricalcium silicate cements, and is responsible for the continuously expanding number of clinical applications of these cements in biomedical tissue engineering (5). Mineral trioxide aggregate (MTA) was developed as a root-end filling material, but its potential for other clinical applications became evident due to its hydraulic properties and sealing ability (6). It is frequently used in several clinical applications, including apical barriers, repair of root perforations, root-end filling, pulpotomy, and direct pulp-capping. It has been also successfully used

in endodontic surgery, apexification, and root resorption (7). The biocompatibility of capping materials, including MTA and calcium hydroxide (CaOH<sub>2</sub>), is an essential factor in the treatment outcome. Both have been shown to be capable of inducing mineralized tissue formation at a variety of dental tissue sites (8). Studies have suggested that the similar clinical response of tooth tissues to both biomaterials is based on a comparable mechanism of action involving the release of calcium and hydroxyl ions (8). MTA is used as a healing material due to its excellent biocompatibility and it is composed mainly of Portland cement, bismuth oxide as a radiopacifier and is considered a calcium silicate-based cement (9) and some brands also contain calcium carbonate.

Pulp capping involves treating an injured pulp after trauma or accidental exposure to preserve the tooth vitality (10). An apical MTA plug improved the repair of the replanted tooth by decreasing surface resorption and repairing mineralized tissue in the periapical region (11). MTA heals pulp by effectively sealing the exposed site (10). This process involves progenitor cell recruitment, proliferation, and differentiation into odontoblast-like cells that secrete a tertiary dentin matrix at the wound site, resulting in dentin bridge formation (12). In this way, treatment with MTA offers major advantages compared to CaOH<sub>2</sub>.

When there is infection, the dentine-pulp complex exhibits significant regenerative response with the tertiary dentine deposited arising from either the original primary

odontoblasts or newly differentiated odontoblast-like cells (13). The differences in complexity of the cellular events involving these two cell populations indicate that the impact of the inflammatory response will have differing effects (13). Despite the therapeutic advantages of MTA and the use in endodontics for the past two decades, there is evidence that some of its molecular components can cause pulp irritation, can induce both M1 and M2 polarization of the RAW 264.7 macrophages and begin a pro-inflammatory reactions and tissue remodeling (14). Then, in the present study, the effects of MTA on the structure and enzymatic activity of sPLA2 was evaluated, shedding light on the cell signaling pathways that mediate pulpal inflammation after capping.

## Material and Methods

### Materials

Snake venom sPLA2 shows structural and physiological similarities with the mammal sPLA2 involved in inflammation (15). Bothrops pirajai (Bp) venom was kindly donated by the Instituto Butantan (São Paulo, Brazil). All solvents and chemical reagents used were purchased from Sigma-Aldrich (St. Louis, MO, USA), Merck (Whitehouse Station, NJ, USA), or Promega (São Paulo, SP, Brazil).

### Purification of sPLA2

Purification of sPLA2 from whole venom was performed as previously described (16). 10 mg of the crude venom were dissolved in 250  $\mu$ l of loading buffer (0.05 M Tris-HCl, pH 8.0) and centrifuged at 4,500 g for 5 min. The supernatant was injected into a BioSuite Q AXC ion exchange column (Waters, Milford, MA, USA). Fractions were eluted with a buffer gradient containing 0.05 M Tris-HCl (pH 8.0) with increasing concentrations of 1.0 M NaCl (0-100%) at a constant flow rate of 1 mL/min. 1 mg of Bp fractions obtained in the first chromatographic step were dissolved in 250  $\mu$ l of aqueous solution containing 0.15% trifluoroacetic acid (TFA). Supernatants were injected into an X-Terra C18 analytical reverse phase column, followed by elution with a mobile phase of 0.15% aqueous TFA with increasing quantities of 66% acetonitrile (0-100%). The purity of sPLA2 was assessed by SDS-PAGE.

### Effect of MTA on Spla2 Chromatography

1 mg of CaOH<sub>2</sub>, p.a., 1 mg of MTA powder (Angelus, Londrina, PR, Brazil), were dissolved in 500  $\mu$ l of loading buffer (0.05 M Tris-HCl, pH 8.0) and incubated for 60 min in the presence of 1 mg of sPLA2. After that, the samples were centrifuged at 4,500 g for 5 min. The supernatant (200  $\mu$ l) was injected into a reverse phase HPLC (66.6% acetonitrile in 0.1% TFA). The oxidation of sPLA2 was determined from an absorption spectrum using a HPLC

(Waters) with a photodiode detector.

### Electrospray Mass (ESI-MS)

The ESI-MS source was used in the positive ionization mode with gas flow at 500 l/m and temperature of 30°C. The spraying gas was adjusted to 30 psi and the temperature kept at 35 °C. The stress cone capillaries were set at 3,000 and 35 V. The samples were obtained from the incubation of 1 mg of CaOH<sub>2</sub>, p.a., 1 mg of MTA powder and 1 mg of sPLA2, diluted in acetonitrile and formic acid for 60 min. After that, the samples were centrifuged at 4,500 g for 5 min. The supernatant (200  $\mu$ l) was injected into ESI-MS.

### Small Angle X-Ray Scattering (SAXS)

SAXS measurements were carried out at the D02A-SAXS2 beamline of the Brazilian Synchrotron Light Laboratory. The samples were prepared as for the other assays. 1 mg of CaOH<sub>2</sub>, p.a., 1 mg of MTA powder and 1 mg of sPLA2 were diluted in distilled water, for 60 min. After that, the samples were centrifuged at 4,500 g for 5 min. Samples were kept at 4 °C in the sample cell and inserted into the apparatus using a 1 ml syringe. Data were acquired by taking several 600ms frames for each sample. Data were collected at a sample-to-detector distance of 985.7 mm using a MAR CCD detector (MAR Research, Fort Lauderdale, FL, USA) with the x-ray at a wavelength of 1.488 Å. The process covered q values from 0.013 to 0.34 Å<sup>-1</sup>, where q, the moment transfer vector, is defined as  $q=4\pi\sin\theta / \lambda$ . Different concentrations of sPLA2 were measured to assess aggregation and interparticle interference effects. The best data sets were collected for samples of native sPLA2 and sPLA2 treated with CaOH<sub>2</sub> p.a., MTA powder and MTA cement (MTA Fillapex, Angelus) at 4 and 7 mg/mL, respectively.

Initial data treatment of the scattering intensities was performed with the Fit2D software package. Data were reduced to a 1D scattering profile and normalized according to intensity and sample attenuation. Net scattered x-ray intensities were determined by subtracting a normalized buffer "blank" sample from each protein data set. Different frames for each sample were inspected and averaged with a Primus software (Version 4.6, Primus software corporation, Duluth, GA, USA). Distance distribution functions, p(r), and radius of gyration, R<sub>g</sub>, were evaluated by the indirect Fourier transform method, as implemented in GNOM software.

The R<sub>g</sub> value was estimated with a Guinier analysis. Briefly, the ln of I(q) was plotted against q<sup>2</sup> to yield a straight line with a slope proportional to R<sub>g</sub>. An additional analysis was performed by plotting Iq<sup>2</sup> versus q (Kratky plot), to evaluate the extent of protein globularization. Molecular weights of sPLA2 and sPLA2-MTA in solution were estimated by a web tool (SAXS MoW v1.0, RV Portugal, <http://www>.

if.sc.usp.br/~saxs/obsolete/obsolete.html). This tool is based on the invariant  $Q$ , as calculated from the Kratky plot.

Crystallographic structures of several sPLA2 molecules found in the Protein Data Bank (PDB, www.rcsb.org) were superimposed with the most probable SAXS models derived from DAMAVER by using SUPCOMB software v.2.3, (ATSAS team). The crystallographic sPLA2 models used in the interpretation of the low-resolution models were chosen based on the smallest discrepancy (chi-squared value) between the experimental scattering data and the

scattering intensities computed for these models using CRY SOL software v.2.8.2 (ATSAS team). Each sample was modeled with iGasbor 20 software. Twenty individual patterns for each set were processed with Damaver software v.5.0 (ATSAS Team), to obtain the average of these models. Rigid-body modeling using SASREF software and flexible-docking modeling using SITUS software v.2.7 (Biomachina.org, New York, NY, USA) were also performed.

## Results

Alterations in the retention time and peak area of sPLA2 were detected by chromatography in the presence of MTA (Fig. 1). ESI-MS provided greater detail regarding the nature and extent of protein modifications of native sPLA2 and sPLA2 incubated with MTA (Fig. 2A and B). These alterations clarify that there is interaction between MTA and PLA2, however, did not elucidate which type of interaction. The data of the interaction between  $\text{CaOH}_2$  and MTA were inconclusive, for that reason not shown.

Figure 3 show the means of SAXS curves for native sPLA2 ( $\circ$ ) and sPLA2 treated with  $\text{CaOH}_2$  ( $\Delta$ ) or with MTA ( $\square$ ). The molecular mass and oligomeric state of the samples were evaluated with the SAXS MoW software. The molecular weights of native sPLA2,  $\text{CaOH}_2$ -treated sPLA2 and MTA-treated sPLA2 were 30.1 kDa (gap, 7.5%), 27.7 kDa (gap, 1.1%) and 30.6 kDa (gap, 1.2%) respectively. In each case, the oligomeric state corresponded to that of a dimer. Figure 4 shows the SAXS models obtained for native sPLA2 (A) and  $\text{CaOH}_2$  (B)- or MTA (C)-treated sPLA2.

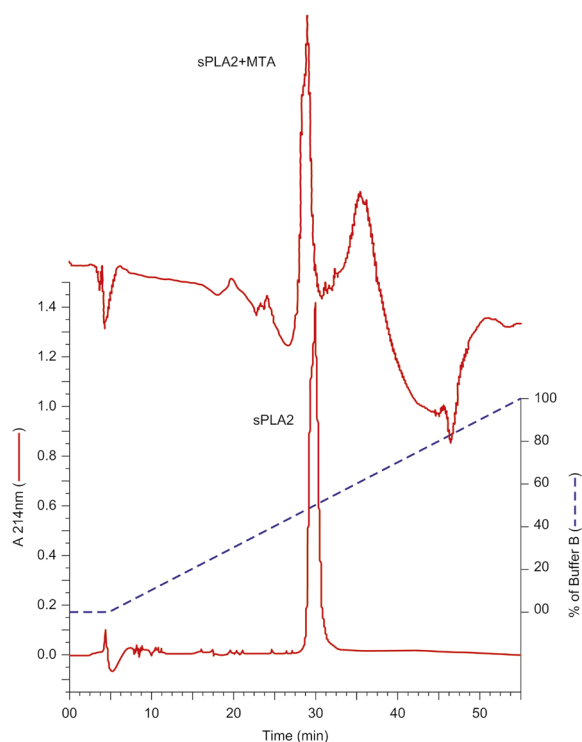


Figure 1. Purification of sPLA2 from the whole venom of *Bothrops pirajai* by reverse phase HPLC. Native sPLA2 incubated with MTA and applied to the column.

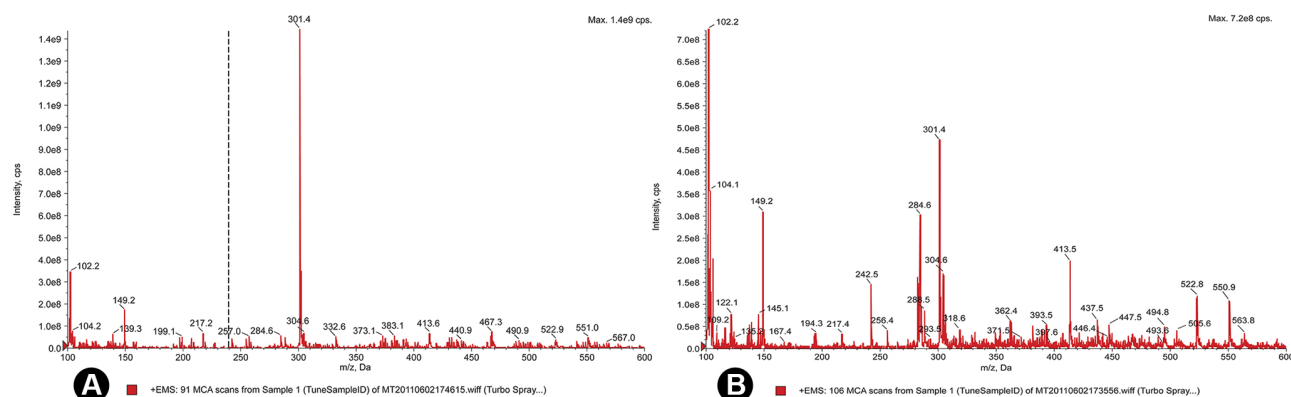


Figure 2. ESI-MS source was used in the positive ionization Native sPLA2 (A) incubated with MTA (B).

process (17). It is believed that calcium hydroxide works as a low-grade irritant to stimulate the formation of hard tissue bridge. Underlying tissues react to irritant by producing collagen, which is partially mineralized; coagulated tissues are calcified, and differentiation of dentine occurs (18).

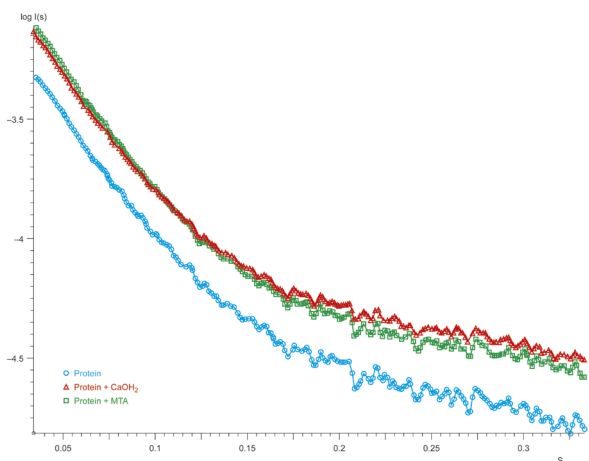


Figure 3. SAXS curves for native sPLA2 (O), CaOH<sub>2</sub>-treated sPLA2 (Δ), and MTA-treated sPLA2 (□).

Sometimes, in spite of dentine bridge formation, chronic inflammation continues, and the pulp becomes necrotic cause of permanency of the inflammatory stimulus (19). In a previous study (20), when MTA ProRoot, MTA Angelus, and white Portland cement were used in furcation perforations of canine premolars without barrier placement in the bone portion of the canal, intensive inflammatory infiltrates were observed after treatment. Moreover, recently have been revealed that sPLA2 activate the inflammatory response through NF-κB signaling, a tumoral marker and through biomineralization (8).

Proteins interact strongly with both synthetic and natural polyelectrolytes (21). Ample evidence exists for the binding of polyanions and polycations to proteins below and above their isoelectric points (21). It is known that calcium can activate sPLA2, as it is attracted by hydrophobic channel of the enzyme (3). sPLA2 belongs to a group of low-molecular-weight secretory enzymes that release phospholipids in early inflammation. sPLA2 catalyzes the hydrolysis of the sn-2 position of membrane glycerophospholipids to liberate arachidonic acid, a precursor of eicosanoids. Due to the molecular weight difference between sPLA2 and CaOH<sub>2</sub>, chromatography and

M.B. Lopes et al.

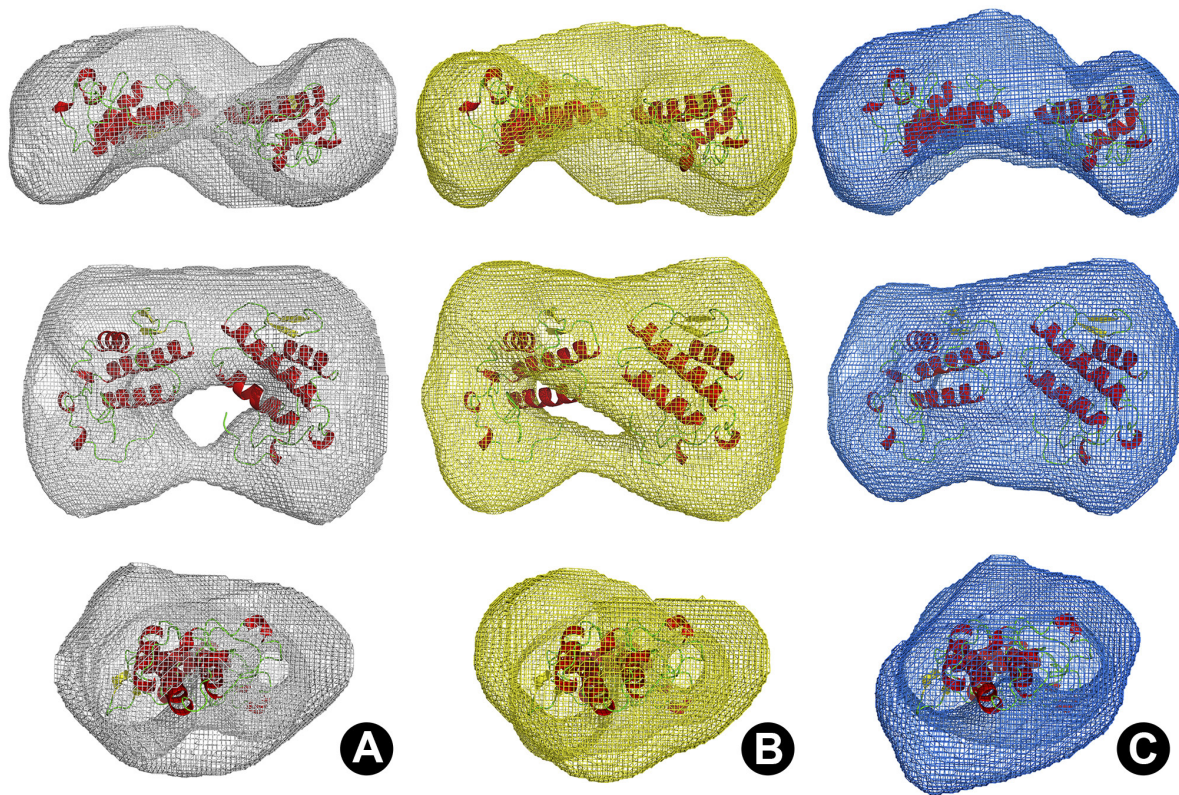


Figure 4 Models obtained by SAXS presented in three different orientations. Models are shown for native sPLA2 (A), CaOH<sub>2</sub>-treated sPLA2 (B), and MTA-treated sPLA2 (C). All models were interpreted with the SAXS dimer constructed in silico from the crystallographic model of Bothrops pirajai (Bp), chains D and F (PDB code: 1BJJ). The figure was prepared using Pymol software v1.5.0 (Delano Scientific LLC, Portland, OG, USA).

ESI-MS can detect disturbances in the molecules; however, these techniques are unable to confirm interactions of the proteins. When SAX, which is a technique that does not separate the components, was used, it was possible to observe that MTA induced modifications on sPLA2 that were like those induced by calcium, which is a cofactor of sPLA2 and may trigger an uncontrolled inflammatory response. Although the chromatography and EMSI assays were performed using the CA as a control because it had a small molecular size, the column used for protein was not able to isolate this molecule, and the data were inconclusive. As the hypothesis was that the calcium present in the MTA was responsible for the enhancement of the immune response caused by its use, the SAX tests were performed, where calcium and protein were in solution and therefore the interaction could become apparent.

Per ESI-MS and SAX analysis, the molecular weight of the native sPLA2 protein was 30.1 kDa. Although the mass after MTA incubation was 27.7 kDa, the signal of ESI-MS was decreased, indicating modification in the protein structure. Moreover, other fragmentation peaks were identified (Fig. 2 - B) that were consistent with possible interactions of sPLA2 with MTA. The changing fragmentation identified by ESI-MS allowed components to be identified, which could approximate the results of inflammation of the MTA to the CaOH<sub>2</sub>. The decreased stability may facilitate the dimer-to-trimer transition.

The SAXS technique was used to demonstrate interactions between sPLA2 and calcium in solution, where the interactions are most clearly preserved (Fig. 3). MTA and CaOH<sub>2</sub> interacted with sPLA2 in a similar fashion due to the presence of calcium. Increasing calcium levels in the cement have been suggested to be related to an increasing inflammatory response (22). The SAX results indicated that presence of calcium on the MTA destabilized the protein to another conformation (Fig. 4), leading to inflammation and may cause necrosis. SAX was also used to determine if the change on the properties of tensile deformation on biomaterials was due to the presence of lauric acid. Similarly, the excess of calcium could be the cause of the protein deformation, which consequently activated the sPLA2 (23). Seminsotnov et al. (24) using SAXS technique showed conformational variation from dimer to trimer, which modified the enzymatic activity, as found in this research.

While MTA has proven to be an effective dental tool, its commercial use is relatively new. According to the patent of MTA (Kerr) (25), a high calcium concentration is used during MTA formulation: tricalcium silicate, dicalcium silicate and tricalcium aluminate. Tricalcium silicate hardens rapidly and is largely responsible for the early strength of Portland cement. Dicalcium silicate has a slower hydration

reaction; it is mostly used to extend the bond strength beyond 1 week. Tricalcium aluminate hydrates rapidly and contributes to early MTA strength development (25). MTA also contains tetracalcium aluminoferrate, bismuth oxide (a radiopaque agent), and hydrated calcium sulfate (gypsum) (26). Its microstructure when hydrated consists of cubic and needle-like crystals. CaOH<sub>2</sub> is the main reaction byproduct of MTA (27).

Although, it is well-know the importance of calcium on the dental remineralization process, our data suggested that excess of calcium might be involved in an increase of the inflammatory response. As there is no need for a great initial strength and a fast setting for pulp sealing materials, the tricalcium silicate may be substituted by dicalcium silicate from the MTA formulation decreasing calcium concentration and consequently reducing sPLA2 activation. Significant interactions between MTA and sPLA2 were showed. MTA induced modifications on sPLA2 that were like those induced by calcium. These findings will aid in our understanding of the mechanisms of action of MTA during the inflammatory process. Calcium was the MTA component that most amplified the inflammatory signal.

## Resumo

O objetivo deste estudo foi analisar os efeitos do MTA na estrutura e atividade enzimática da sPLA2 a fim de fornecer subsídios para melhoria na formulação do produto. O MTA em pó foi incubado por 60 min na presença de sPLA2 e analisado por cromatografia, espectroscopia de massa por eletropulverização (ESI-MS) e espalhamento de raios-X de baixo ângulo (SAXS). Encontrou-se que o perfil de eluição, o tempo de retenção e a fragmentação da sPLA2 foram alterados após o tratamento com MTA. O cálcio foi o componente do MTA que mais ampliou o sinal inflamatório. Encontraram-se interações significativas entre o MTA e o sPLA2, o que poderia auxiliar na compreensão dos mecanismos de ação do MTA durante o processo inflamatório e facilitar a modificação estrutural do MTA, melhorando sua segurança biológica e consequentemente a taxa de sucesso do tratamento.

## Acknowledgements

The authors wish to thank the National Laboratory of Synchrotron Light (LNLS - Brazil) for the use of their facility and equipment and to Brazilian division of the IADR (SBPqO), which partially supported this study through PRONAC award. The authors also thanks to Prof. Marcos Toyama for its support on the chromatography graphs.

## References

1. Lara Vde P, Cardoso FP, Brito LC, Vieira LQ, Sobrinho AP, Rezende TM. Experimental Furcal Perforation Treated with MTA: Analysis of the Cytokine Expression. *Braz Dent J* 2015;26:337-341.
2. Pääkkönen V, Ohlmeier S, Bergmann U, Larmas M, Salo T, Tjäderhane L. Analysis of gene and protein expression in healthy and carious tooth pulp with cDNA microarray and two-dimensional gel electrophoresis. *Eur J Oral Sci* 2005;113:369-379.
3. Murakami MT, Viçoti MM, Abrego JR, Lourenzoni MR, Cintra AC, Arruda EZ. Interfacial surface charge and free accessibility to the PLA2-active site-like region are essential requirements for the activity of Lys49 PLA2 homologues. *Toxicon* 2007;49:378-387.
4. Odijk T. Protein-macromolecule interactions. *Macromolecules*

- 1996;29:1842-1843.
5. Eid AA, Hussein KA, Niu LN, Li GH, Watanabe I, Al-Shabrawey M. Effects of tricalcium silicate cements on osteogenic differentiation of human bone marrow-derived mesenchymal stem cells in vitro. *Acta Biomater* 2014;10:3327-3334.
  6. Prati C, Gandolfi MG. Calcium silicate bioactive cements: Biological perspectives and clinical applications. *Dent Mater* 2015;31:351-370.
  7. Bernabé PF, Gomes-Filho JE, Bernabé DG, Nery MJ, Otoboni-Filho JA, Dezan E Jr. Sealing ability of MTA used as a root end filling material: effect of the sonic and ultrasonic condensation. *Braz Dent J* 2013;24:107-110.
  8. Reyes-Carmona JF, Santos AR, Figueiredo CP, Felipe MS, Felipe WT, Cordeiro MM. In vivo host interactions with mineral trioxide aggregate and calcium hydroxide: inflammatory molecular signaling assessment. *J Endod* 2011;37:1225-1235.
  9. Gomes-Cornélio AL, Rodrigues EM, Salles LP, Mestieri LB, Faria G, Guerreiro-Tanomaru JM. Bioactivity of MTA Plus, Biodentine and an experimental calcium silicate-based cement on human osteoblast-like cells. *Int Endod J* 2017;50:39-47.
  10. Tran XV, Gorin C, Willig C, Baroukh B, Pellat B, Decup F. *J Dent Res* 2012;91:1166-1171.
  11. Esteves JC, Marão HF, Silva PI, Poi WR, Panzarini SR, Aranega AM. Delayed tooth replantation following root canal filling with calcium hydroxide and MTA: Histomorphometric study in rats. *Arch Oral Biol* 2015;60:1254-1262.
  12. Bjorndal L, Mjor IA. Pulp-dentin biology in restorative dentistry. Part 4: Dental caries--characteristics of lesions and pulpal reactions. *Quintessence Int* 2001;32:717-736.
  13. Cooper PR, Takahashi Y, Graham LW, Simon S, Imazato S, Smith AJ. Inflammation-regeneration interplay in the dentine-pulp complex. *J Dent* 2010;38:687-697.
  14. Zhu X, Yuan Z, Yan P, Li Y, Jiang H, Huang S. Effect of iRoot SP and mineral trioxide aggregate (MTA) on the viability and polarization of macrophages. *Arch Oral Biol* 2017;80:27-33.
  15. Murakami M, Taketomi Y, Sato H, Yamamoto K. Secreted phospholipase A2 revisited. *J Biochem* 2011;150:233-255.
  16. dos Santos ML, Fagundes FH, Teixeira BR, Toyama MH, Aparicio R. Purification and preliminary crystallographic analysis of a new Lys49-PLA2 from *B. Jararacussu*. *Int J Mol Sci* 2008;9:736-750.
  17. Silveira RL, Machado RA, Silveira CR, Oliveira RB. Bone repair process in calvarial defects using bioactive glass and calcium sulfate barrier. *Acta Cir Bras* 2008;23:322-328.
  18. Higashi T, Okamoto H. Characteristics and effects of calcified degenerative zones on the formation of hard tissue barriers in amputated canine dental pulp. *J Endod* 1996;22:168-172.
  19. Gudkina J, Mindere A, Locane G, Brinkmane A. Review of the success of pulp exposure treatment of cariously and traumatically exposed pulps in immature permanent incisors and molars. *Stomatologija* 2012;14:71-80.
  20. Juárez Broon N, Bramante CM, de Assis GF, Bortoluzzi EA, Bernardineli N. Healing of root perforations treated with mineral trioxide aggregate (MTA) and Portland cement. *J App Oral Sci* 2006;14:305-311.
  21. Park JM, Muhoberac BB, Dubin PL, Xia JL. Effects of Protein Charge Heterogeneity in Protein-Polyelectrolyte Complexation. *Macromolecules* 1992;25:290-295.
  22. Ruller R, Aragão EA, Chioato L, Ferreira TL, de Oliveira AH, Sà JM. A predominant role for hydrogen bonding in the stability of the homodimer of bothropstoxin-I, A lysine 49-phospholipase A2. *Biochimie* 2005;87:993-1003.
  23. Renouf-Glauser AC, Rose J, Farrar D, Cameron RE. A degradation study of PLLA containing lauric acid. *Biomaterials* 2005;26:2415-2422.
  24. Semisotnov GV, Kihara H, Kotova NV, Kimura K, Amemiya Y, Wakabayashi K. Protein globularization during folding. A study by synchrotron small-angle X-ray scattering. *J Mol Biol* 1996;262:559-574.
  25. Torabinejad M, White DJ. Tooth filling material and method of use. USA: Loma Linda University 1995.
  26. Hashiguchi D, Fukushima H, Yasuda H, Masuda W, Tomikawa M, Morikawa K. Mineral trioxide aggregate inhibits osteoclastic bone resorption. *J Dent Res* 2011;90:912-917.
  27. Camilleri J. Characterization of hydration products of mineral trioxide aggregate. *Int Endod J* 2008;41:408-417.

Received March 11, 2019  
Accepted April 22, 2019